

Holistic Ecosystem Dynamics with Lampreys Considering Age Structure and Diffusion Terms

Summary

Sex ratio of lampreys has significant impacts on marine ecosystem, and we have been tasked to verify this claim. Therefore, the holistic ecosystem dynamics considering age structure and parasite distribution dynamics with diffusion terms are established based on nonlinear dynamics and equilibrium points theory.

To begin with, the entire marine ecosystem is divided into six compartments. Crucially, the holistic ecosystem dynamics considering age structure is established to describe the relationship between each category. Then, polynomial regression and support vector machines are both applied to construct the sex ratio function. To express the instantaneous pulse of the lamprey maturation and death functions, Dirac Delta function is introduced. Finally, characteristic line and finite differential method are utilized to simulate the dynamics and analyze the visualisation results.

Next, in order to analyze the Lyapunov steady states, trivial and semi-trivial equilibrium points are computed theoretically. Due to the complexity of the system, Levenberg-Marquardt algorithm and Trust Region Policy Optimization algorithm are respectively applied to solve the semi-trivial equilibrium points numerically. In addition, we draw its phase diagrams and discuss the special nontrivial equilibrium points when the age function is a constant.

When taking the relationship between parasites and lamprey sex ratio into account, a two-dimensional second-order partial differential equation with diffusion terms is added to the original dynamics. On the basis of Chebyshev Spectral Method, the distribution of parasites affected by sex ratio is simulated numerically. We discover that the diffusion rate is positively correlated with the diffusion coefficient. Besides, the density field tends to stabilize over a long period of time. Thus, the dynamics can be transformed into Laplace equation.

What's more, in sensitivity analysis, we find that the level of parasite density is strongly related to the initial value conditions. To ensure the accuracy of sex ratio function, we calculate the determination coefficient by data set from NOAA. After stating the strengths and weaknesses of the model, the latest research results and directions are mentioned in future discussion.

Keywords: sex ratio; age-structured; equilibrium point; Chebyshev Spectral Method

Contents

1	Introduction	3
1.1	Background	3
1.2	Problem Restatement	3
1.3	Our Work	4
2	Assumptions and Justifications	4
3	Notations	5
4	Holistic Ecosystem Dynamics Considering Age Structure	6
4.1	Division of Ecosystem and Basic Mathematical Model	6
4.2	Further Discussion on Sex Ratio Function	10
4.3	Characteristic Line and Dirac Delta Function	11
4.4	Numerical Simulation and Results Analysis	12
5	Equilibrium Points and the Steady States	17
5.1	Derivation of Trivial and Semi-trivial Equilibrium Points	17
5.2	Non-trivial Equilibrium Points and Phase Diagram	18
6	Parasite Distribution Dynamics with Diffusion Terms	20
6.1	Sex Ratio and Parasite Distribution Model	20
6.2	Numerical Simulation and Chebyshev Spectral Method	21
7	Sensitivity Analysis and Model Testing	23
8	Strengths and Weaknesses	24
8.1	Strengths	24
8.2	Weaknesses	24
9	Future Discussion	24
References		25

1 Introduction

1.1 Background

The sea lamprey is a species with an uneven sex ratio. In the larval stage, they are not sex-specific, but at maturity, due to external environmental influences, they exhibit changes in sex ratios. Specifically, the greater the availability of food, the slower the larval growth rate for males and the higher for females, yet the proportion of males always remains higher than that of females^[1].

Additionally, lampreys have no natural predators, but they attack other species by attaching to them after maturation, hence their population can impact the ecosystem, resulting in a series of advantages and disadvantages.

1.2 Problem Restatement

Given the context and constraints outlined in the background, we are tasked with addressing the following concerns:

- Build a model to figure out how the ability of lampreys to adjust their sex ratios impact the wider ecological system. This model should examine the direct and indirect effects on biodiversity, food chains, and ecological balance.
- Analyze the pros and cons for the lamprey population as a result of their adjustments in sex ratio.
- Discover the implications of alterations in the gender distribution of lampreys for the overall stability and health of the ecosystem. This exploration should aim to identify how these alterations affect the dynamics between predator and prey, impact the reproductive success of the species, and influence the ecological balance.
- Find out whether other members of the ecosystem, like parasites, can benefit from the variability in the sex ratios of the lamprey population.

1.3 Our Work

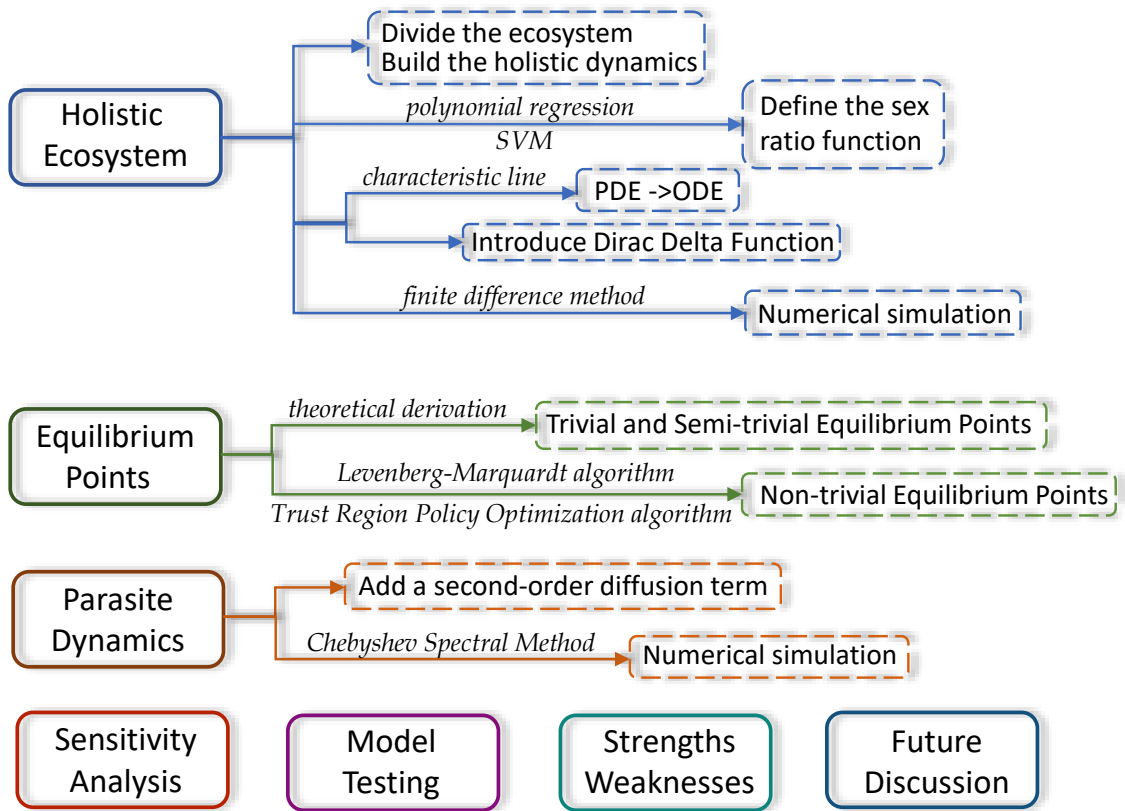


Figure 1: The flowchart of our work

In this paper, we establish **two** mathematical models progressively, which are listed below:

- Holistic ecosystem dynamics considering age structure.
- Parasite distribution dynamics with diffusion terms.

Besides, we also analyze the ODE-PDE dynamics from numerical simulations (Finite Difference Method and Chebyshev Spectral Method), equilibrium points (Levenberg-Marquardt algorithm and Trust Region Policy Optimization algorithm) and its sensitivity.

2 Assumptions and Justifications

In order to simplify the issues, we make the following assumptions, each of which is supported by justification. Assumption 1 and 2 are applied to section 4. Assumption 3 is applied to section 6.

Assumption 1. Lampreys will be mature with the availability of spawning and attacking other species at the age of 5, and the total life span is approximately 6 years old.

→ *Justification:* According to [2], sexual maturity is reached in the first spring following metamorphosis, when the adult spawns and dies. The metamorphosis is occurred when the lamprey is four and a half years old to five and a half years old. The total life span of lamprey is exactly six years old.

Assumption 2. Lamprey has only one spawning period, and both male and female will die immediately after spawning.

→ *Justification:* [3] tells us that at least 41 species of existing lampreys are acknowledged; each undergoes semelparity, dying after a single spawning season (although not necessarily after a single spawning event), and all spawn in freshwater.

Assumption 3. After metamorphosis, lampreys become aggressive and parasitic.

→ *Justification:* According to [4], by determining whether or not they can parasitize, lamprey can be divided into two categories: parasitic and non-parasitic (brook) lampreys.

3 Notations

Parameters that appear multiple times in the document are listed in table 1.

Table 1: **Notations used in this paper**

Symbol	Definition	Unit
Z	the population of Plankton	–
P	the population of Zooplanktivorous fish	–
V	the population of Piscivorous fish	–
L	the population of Larval lampreys	–
$S^{(1)}$	the population of Male lampreys with attack and spawning properties	–
$S^{(2)}$	the population of Female lampreys with attack and spawning properties	–
μ	the death rate of various species	%
r	the inherent growth rate of various species	%
K	the maximum environmental capacity of various species	–
$\sigma_{b \rightarrow a}$	the consumption rate of species a by species b	%
A_1	the earliest age that lampreys are capable of reproduction	–
A_2	the maximum life span of lampreys	–
u	the density of parasites at specific location and time	–
F	the function is used to determine sex ratio of lampreys	–

4 Holistic Ecosystem Dynamics Considering Age Structure

4.1 Division of Ecosystem and Basic Mathematical Model

In this part, we make a finite division of the holistic ecosystem where the lampreys live and establish a differential dynamical system considering age structure that can describe the process of change in the holistic ecosystem.

Based on the nature of marine ecosystem, we divide the entire population into six compartments namely: $Z(t)$ – Plankton, $P(t)$ – Zooplanktivorous fish (*i.e.* fish that eat plankton), $V(t)$ – Piscivorous fish (*i.e.* fish that eat zooplanktivorous fish), $L(t, a)$ – Larvae of lampreys (without attack and spawning properties), $S^{(1)}(t, a)$ – Male lampreys with attack and spawning properties and $S^{(2)}(t, a)$ – the counterparts of Female lampreys. (as Figure 2 shown)

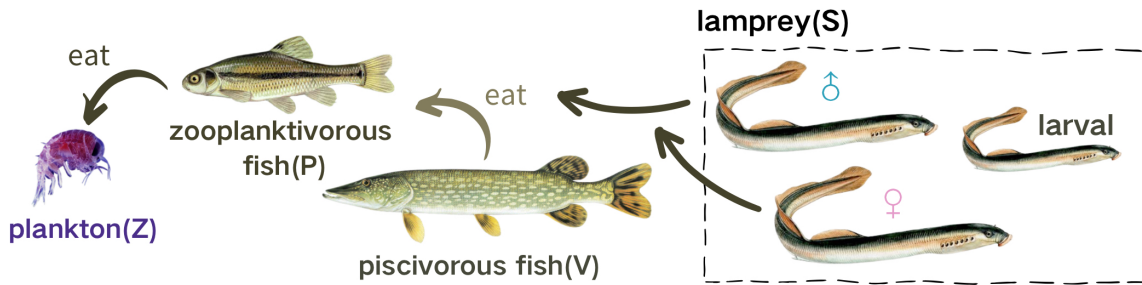


Figure 2: Division of Ecosystem (schematic diagram)

The growth flux is recruited into the plankton $Z(t)$ compartment by the rate $r_z Z(t) \left[1 - \frac{Z(t)}{K_z}\right]$ which follows the logistic law. Besides, it decreases by the natural death $\mu_z Z(t)$ and the consumption by Zooplanktivorous fish $\sigma_{p \rightarrow z} Z(t) P(t)$. Clearly, changes in plankton over time can be expressed as

$$\frac{dZ(t)}{dt} = r_z Z(t) \left[1 - \frac{Z(t)}{K_z}\right] - \mu_z Z(t) - \sigma_{p \rightarrow z} Z(t) P(t), \quad (1)$$

where

μ_z is the natural death rate of plankton;

r_z is the inherent growth rate of plankton;

K_z is the maximum environmental capacity for plankton;

$\sigma_{p \rightarrow z}$ is the consumption rate of plankton by zooplanktivorous fish.

The population of zooplanktivorous fish increases with force of inherent logistic growth and decreases by four main parts: natural death, the consumption by Piscivo-

rous fish, male and female lampreys with attack and breeding properties. Compliant individuals can be expressed through integrals $\int_{A_1}^{A_2} S^{(i)}(t, a)da$ ($i = 1, 2$). The variable Ψ is used to simplify the equation and has no real meaning. Clearly, changes in zooplanktivorous fish over time can be expressed as

$$\begin{aligned}\frac{dP(t)}{dt} &= r_p P(t) \left[1 - \frac{P(t)}{K_p} \right] - \mu_p P(t) - P(t) \cdot \Psi, \\ \Psi &= \sigma_{v \rightarrow p} V(t) + \sum_{i=1}^2 \left[\sigma_{s^{(i)} \rightarrow p} \int_{A_1}^{A_2} S^{(i)}(t, a)da \right],\end{aligned}\tag{2}$$

where

μ_p is the natural death rate of zooplanktivorous fish;

r_p is the inherent growth rate of zooplanktivorous fish;

K_p is the maximum environmental capacity for zooplanktivorous fish;

$\sigma_{v \rightarrow p}$ is the consumption rate of zooplanktivorous fish by Piscivorous fish;

$\sigma_{s^{(i)} \rightarrow p}$ is the consumption rate of zooplanktivorous fish by compliant lampreys;

A_1 is the earliest age that lampreys are capable of reproduction (**assumption 1**);

A_2 is the maximum life span of lampreys (**assumption 1**).

Similarly, the population of Piscivorous fish also increases with force of inherent logistic growth but the difference is that it decreases by only three main parts without predator attack compared with the zooplanktivorous one. The variable Ψ is used to simplify the equation again and has no real meaning. Clearly, changes in Piscivorous fish over time can be expressed as

$$\begin{aligned}\frac{dV(t)}{dt} &= r_v V(t) \left[1 - \frac{V(t)}{K_v} \right] - \mu_v V(t) - V(t) \cdot \Psi, \\ \Psi &= \sum_{i=1}^2 \left[\sigma_{s^{(i)} \rightarrow v} \int_{A_1}^{A_2} S^{(i)}(t, a)da \right],\end{aligned}\tag{3}$$

where

μ_v is the natural death rate of Piscivorous fish;

r_v is the inherent growth rate of Piscivorous fish;

K_v is the maximum environmental capacity for Piscivorous fish;

$\sigma_{s^{(i)} \rightarrow p}$ is the consumption rate of Piscivorous fish by compliant lampreys.

Since larvae of lampreys do not develop the suckers which are a necessity for attack, have no ability to reproduce and are not sexually distinct, we discuss them as a separate category. By **assumption 2**, the number of larvae is determined by the

number of female adult lampreys, and whether female adult lampreys are capable of reproducing is closely related to their age, so we take age a as an independent variable into consideration.

It is clear that the larvae of lampreys can be expressed as a partial differential equation (4) with a Dirichlet boundary value condition (5):

$$\frac{\partial L(t, a)}{\partial t} + \frac{\partial L(t, a)}{\partial a} = -\mu_l \cdot L(t, a), \quad 0 \leq a \leq A_1, \quad (4)$$

$$L(t, 0) = \varepsilon \cdot \int_{A_1}^{A_2} \beta(a) \cdot S^{(2)}(t, a) da, \quad (5)$$

where

μ_l is the natural death rate of larvae of lampreys;

$\beta(a)$ describes the reproductive capacity changing with age (section 4.3);

ε is the number of larvae that a female lamprey can successfully breed with.

After a period of time, larvae of lampreys develop into adults with reproduction ability. $L(t, A_1)$ represents the end of the larval stage. Now the question is transformed into how to differentiate between the sexes of these individuals.

Since the sex ratio is closely related to the food and nutrition in nature (*i.e.* zooplanktivorous fish and Piscivorous fish), we introduce a bounded control function $F(P(t), V(t))$ with a value ranging between 0 and 1. More details about sex ratio control function, you can refer to the following section 4.2. Thus, the male and female lampreys with attack and breeding properties can be expressed as equation (6) and (7) respectively where $A_1 < a \leq A_2$.

$$\nabla S^{(1)}(t, a) = F(P(t), V(t)) \cdot L(t, A_1) - \mu_{S^{(1)}}(a) S^{(1)}(t, a), \quad (6)$$

$$\nabla S^{(2)}(t, a) = [1 - F(P(t), V(t))] \cdot L(t, A_1) - \mu_{S^{(2)}}(a) S^{(2)}(t, a), \quad (7)$$

where

∇ is the first order linear operator and $\nabla = \frac{\partial}{\partial t} + \frac{\partial}{\partial a}$;

$\mu_{S^{(i)}}(a)$ ($i = 1, 2$) describes the death rate changing with age (section 4.3).

In order to promise that the differential equations are well-posed and have practical significance, some initial value conditions are given out

$$\begin{aligned}
Z(0) &= Z_0 \geq 0, & P(0) &= P_0 \geq 0, & V(0) &= V_0 \geq 0, \\
L(0, a) &= L_0(a) \in \mathcal{L}^1([0, A_1], \mathbb{R}), \\
S^{(1)}(0, a) &= S_0^{(1)}(a) \in \mathcal{L}^1((A_1, A_2], \mathbb{R}), \\
S^{(2)}(0, a) &= S_0^{(2)}(a) \in \mathcal{L}^1((A_1, A_2], \mathbb{R}),
\end{aligned}$$

where $\mathcal{L}^1(I, \mathbb{R})$ represents all Lebesgue integrable functions on interval I .

The schematic diagram of changes of the state variables is illustrated in Figure 3. By equation (1) to (7), the dynamic model of ecosystem with lampreys is described by the age-structured equations:

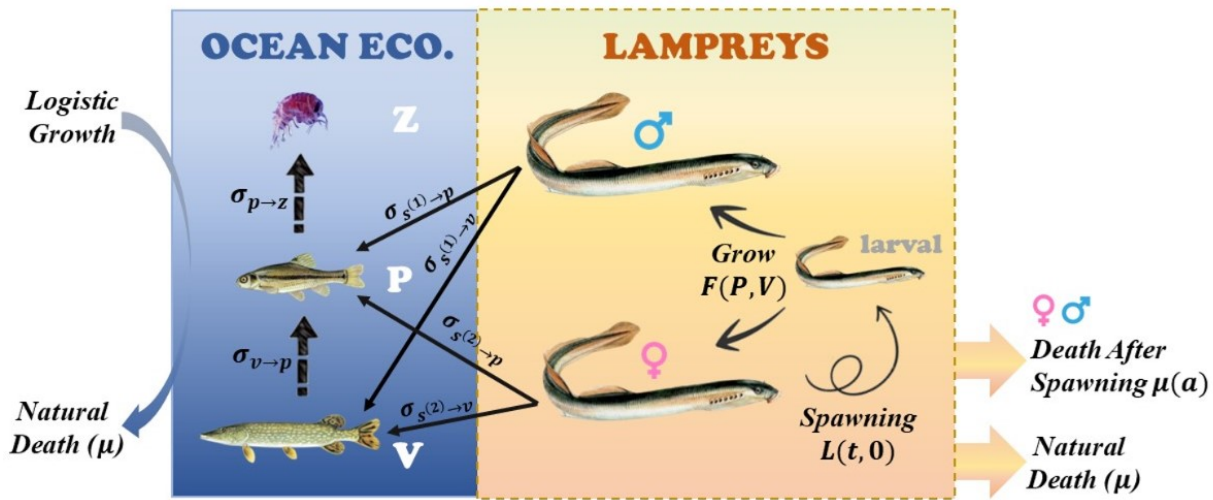


Figure 3: The flowchart of dynamic model of ecosystem with lampreys

$$\left\{
\begin{aligned}
\frac{dZ(t)}{dt} &= r_z Z(t) \left[1 - \frac{Z(t)}{K_z} \right] - \mu_z Z(t) - \sigma_{p \rightarrow z} Z(t) P(t), \\
\frac{dP(t)}{dt} &= r_p P(t) \left[1 - \frac{P(t)}{K_p} \right] - \mu_p P(t) - P(t) \left\{ \sigma_{v \rightarrow p} V(t) + \sum_{i=1}^2 \left[\sigma_{s^{(i)} \rightarrow p} \int_{A_1}^{A_2} S^{(i)}(t, a) da \right] \right\}, \\
\frac{dV(t)}{dt} &= r_v V(t) \left[1 - \frac{V(t)}{K_v} \right] - \mu_v V(t) - V(t) \left\{ \sum_{i=1}^2 \left[\sigma_{s^{(i)} \rightarrow v} \int_{A_1}^{A_2} S^{(i)}(t, a) da \right] \right\}, \\
\nabla L(t, a) &= -\mu_l \cdot L(t, a), & 0 \leq a \leq A_1, \\
\nabla S^{(1)}(t, a) &= F(P(t), V(t)) \cdot L(t, A_1) - \mu_{S^{(1)}}(a) S^{(1)}(t, a), & A_1 < a \leq A_2, \\
\nabla S^{(2)}(t, a) &= [1 - F(P(t), V(t))] \cdot L(t, A_1) - \mu_{S^{(2)}}(a) S^{(2)}(t, a), & A_1 < a \leq A_2,
\end{aligned} \right. \quad (8)$$

with the Dirichlet boundary value condition:

$$L(t, 0) = \varepsilon \cdot \int_{A_1}^{A_2} \beta(a) \cdot S^{(2)}(t, a) da,$$

and the initial value conditions:

$$\left\{ \begin{array}{l} Z(0) = Z_0 \geq 0, \quad P(0) = P_0 \geq 0, \quad V(0) = V_0 \geq 0, \\ L(0, a) = L_0(a) \in \mathcal{L}^1([0, A_1], \mathbb{R}), \\ S^{(1)}(0, a) = S_0^{(1)}(a) \in \mathcal{L}^1((A_1, A_2], \mathbb{R}), \\ S^{(2)}(0, a) = S_0^{(2)}(a) \in \mathcal{L}^1((A_1, A_2], \mathbb{R}). \end{array} \right.$$

It is assumed that all the constant parameters in the model are positive, and all the age-dependent parameters are non-negative, bounded and piece-wise continuous functions on $[0, A_2]$.

4.2 Further Discussion on Sex Ratio Function

In this part, literature review on lampreys sex ratio and overall environmental biomass is made. Then, polynomial regression and support vector machines are both applied to deal with the relationship between the sex ratio of lampreys and the number of trout in the Great Lakes region (Superior) of North America from 1995 to 2019.

Beginning with the publication of the first paper examining the spawning habits of the lamprey in 1898^[5], there have been an increasing number of articles studying various aspects of the lamprey. From reading the papers, we have learned that the sex ratio of the lamprey is generally more male than female, and that the percentage of male decreases as the overall number of lamprey increases^[1]. Moreover, environmental factors can influence sex determination during the process of larvae becoming mature. The productive stream environment will let sex ratios become less skewed towards males, while conversely in unproductive lentic environments, environmental features resulted in further skewing of sex ratios^[6].

To find out how the lamprey sex ratio affects the overall ecology, we visit *Great Lakes Fishery Commission*¹ to search for relevant data and found the *Sea Lamprey Control In The Great Lakes* report from 2011-2019 and *Integrated Management Of Sea Lampreys In The Great Lakes* from 1995-2010^[4]. The lamprey sex ratio and the lake trout marking rate by lamprey attack for each lake are recorded in the annual report. Due to COVID-19 in 2020, we intercepted the average male percent rate and lake trout marking rate for Superior Lake of the Great Lakes each year from 1995-2019.

First, we clean the data from the discrete points and remove outliers based on the Quartile range to obtain a box plot. Then, polynomial regression and machine learning algorithm: support vector machines are used to fit the data, respectively.

¹Great Lakes Fishery Commission: <http://www.glfcc.int/> accessed on Feb.5th, 2024

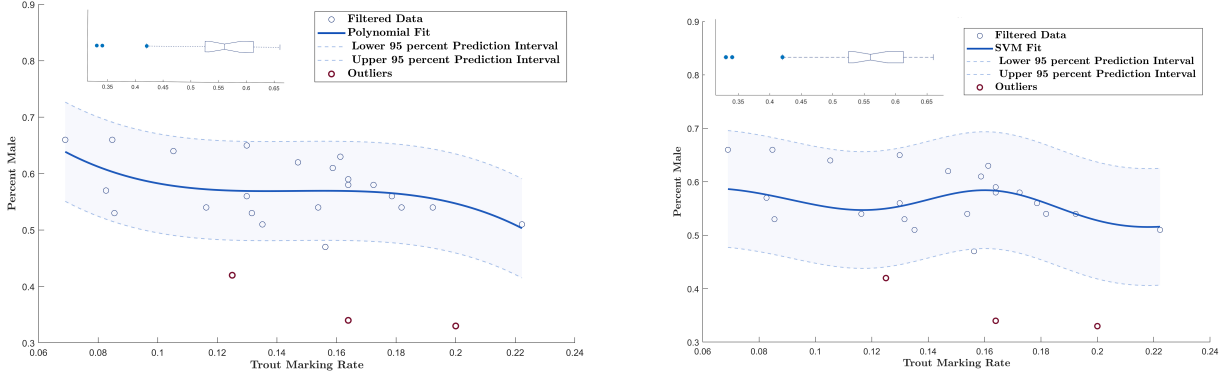


Figure 4: Outliers and curve fitting: polynomial regression (left) and support vector machines (right)

The results of curve fitting are shown in figure 4. After computing the mean-square error (MSE) of each method, we find that $MSE = 0.0021$ for polynomial regression and $MSE = 0.0031$ for Support vector machines algorithm. Therefore, we retain the result of polynomial regression: $F = -158.10x^3 + 69.35x^2 - 10.09x + 1.06$.

4.3 Characteristic Line and Dirac Delta Function

In this part, since the partial differential operator ∇ is linear, characteristic line is applied to transform PDEs into ODEs. Besides, function $\beta(a)$ and $\mu_{s(i)}(a)$ left over from section 4.1 will also be addressed in this part.

For $L(t, a)$, we can solve along the characteristic line $a = t + c$, where c is a constant. Define $w_c(t) \triangleq L(t, t + c)$, $t > t_c$, where $t_c = \max\{0, -c\}$. Therefore, the equation (4) can be rewritten as (9) as below:

$$\frac{dw_c(t)}{dt} = -\mu_l \cdot w_c(t), \quad t \geq t_c. \quad (9)$$

It is not difficult to give out the general solution of equation (9):

$$w_c(t) = w_c(t_c) e^{-\mu_l(t-t_c)}.$$

Eventually, we can get a simple expression for the segmented $L(t, a)$:

$$L(t, a) = \begin{cases} L(0, a - t) e^{-\mu_l t} & , a \geq t, \\ L(t - a, 0) e^{-\mu_l a} & , a < t. \end{cases}$$

Due to space constraints, the same approach can be used for transforming the equation (6) and (7) to ordinary differential equations, so we will not give specific calculation process and results here.

In section 4.1, we have already defined the reproductive capacity function $\beta(a)$ and the death rate function $\mu_{S^{(i)}}(a)$ ($i = 1, 2$) without giving the specific graphs. By **assumption 1**, since lamprey will be mature with the availability of breeding and attacking other species at the age of 5, the reproductive capacity function is jump-interrupted at $a = 5$. By **assumption 2**, since both male and female will die immediately after spawning, the death rate function is jump-interrupted, with almost 100 per cent mortality after reproduction.

Here we introduce the generalized function: Dirac Delta Function $\delta(x)$, which satisfies $\int_E \delta(x)dx \rightarrow 1$ ($E = [0, A_2]$ is domain). Thus,

$$\beta(a) = \mu_{S^{(i)}}(a) = \begin{cases} 1, & |a - \frac{A_1+A_2}{2}| \leq \frac{A_2-A_1}{2}, \\ \mu_l, & |a - \frac{A_1+A_2}{2}| > \frac{A_2-A_1}{2}, \end{cases}$$

where $\beta(a)$ and $\mu_{S^{(i)}}(a)$ ($i = 1, 2$) are Dirac Delta function.

4.4 Numerical Simulation and Results Analysis

In this part, we simulate the dynamics of the ecosystem and analyze the visualisation results. In order to compute the ordinary-partial differential equations system (8), the *Finite Difference Method* is applied which is based on the principle that the derivative at a point can be approximated by the slope of the secant line through that point and a nearby point. Suppose that age step and time step are denoted as da and dt , we have

$$\begin{aligned} Z_n &= Z_{n-1} + dt \left[r_z Z_{n-1} \left(1 - \frac{Z_{n-1}}{K_z} \right) - \mu_z Z_{n-1} - \sigma_{p \rightarrow z} Z_{n-1} P_{n-1} \right], \\ P_n &= P_{n-1} + dt \left[r_p P_{n-1} \left(1 - \frac{P_{n-1}}{K_p} \right) - \mu_p P_{n-1} - \sigma_{v \rightarrow p} P_{n-1} V_{n-1} - \sum_{i=1}^2 \sigma_{s^{(i)} \rightarrow p} P_{n-1} I_{s_i} \right], \\ V_n &= V_{n-1} + dt \left[r_v V_{n-1} \left(1 - \frac{V_{n-1}}{K_v} \right) - \mu_v V_{n-1} - \sum_{i=1}^2 \sigma_{s^{(i)} \rightarrow v} V_{n-1} I_{s_i} \right], \\ L_{i,n} &= L_{i,n-1} - dt \left[\mu_l L_{i,n-1} + (L_{i,n-1} - L_{i-1,n-1}) \frac{1}{da} \right], \\ S_{i,n}^{(1)} &= S_{i,n-1}^{(1)} - dt \left[F \cdot L_{n-1} - \mu_{S^{(1)}} S_{i,n-1}^{(1)} - \left(S_{i,n-1}^{(1)} - S_{i-1,n-1}^{(1)} \right) \frac{1}{da} \right], \\ S_{i,n}^{(2)} &= S_{i,n-1}^{(2)} - dt \left[(1 - F) \cdot L_{n-1} - \mu_{S^{(2)}} S_{i,n-1}^{(2)} - \left(S_{i,n-1}^{(2)} - S_{i-1,n-1}^{(2)} \right) \frac{1}{da} \right], \end{aligned}$$

where I_{s_i} ($i = 1, 2$) are numerical integration.

Then we assigned values to the parameters and used discrete form to solve for the dynamics of the ecosystem.

Table 2: **Parametric description and their values**

Parameter	Description	Values	Sources
r_z	the inherent growth rate of plankton	32	[7]
r_p	the inherent growth rate of zooplanktivorous fish	22	[7]
r_v	the inherent growth rate of Piscivorous fish	2	[7]
μ_z	the death rate of plankton	0.05	assumed
μ_p	the death rate of zooplanktivorous fish	0.02	assumed
μ_v	the death rate of Piscivorous fish	0.01	assumed
μ_l	the death rate of larval lamprey	0.05	[4]
K_z	the maximum environmental capacity of plankton	5000	assumed
K_p	the maximum environmental capacity of zooplanktivorous fish	2000	assumed
K_v	the maximum environmental capacity of Piscivorous fish	1000	assumed
$\sigma_{p \rightarrow z}$	the consumption rate of plankton by zooplanktivorous fish	0.02	[7]
$\sigma_{v \rightarrow p}$	the consumption rate of zooplanktivorous fish by Piscivorous fish	0.01	[7]
$\sigma_{s^{(1)} \rightarrow p}$	the consumption rate of zooplanktivorous fish by male lampreys	0.01	assumed
$\sigma_{s^{(2)} \rightarrow p}$	the consumption rate of zooplanktivorous fish by female lampreys	0.01	assumed
$\sigma_{s^{(1)} \rightarrow v}$	the consumption rate of Piscivorous fish by male lampreys	0.02	assumed
$\sigma_{s^{(2)} \rightarrow v}$	the consumption rate of Piscivorous fish by female lampreys	0.02	assumed
A_1	earliest age that lampreys are capable of reproduction	5	[2]
A_2	the maximum life span of lampreys	6	[2]
ε	number of larvae that a female lamprey can successfully spawn	12	[4]

Table 3: **Illustration of the MATLAB Simulation****Input:**Parameters: $r, \mu, \sigma, K, A_1, A_2, \varepsilon$ Initial value conditions: L, Z, P, V, S_1, S_2 **While:** Traverse from 2 to 1000 in steps of 1**Main script:**

- Upgrade $Z(n)$, $P(n)$ and $V(n)$ by using the formula obtained above.
- **For:** Traverse lamprey's larval period from born to age 5
- Upgrade $L(i,n)$ by using the formula obtained above.
- **For:** Traverse lamprey's maturation period from age 5 to 6
- Upgrade $S_1(j,n)$ and $S_2(j,n)$ by using the formula obtained above.
- Calculate the Dirichlet boundary value condition $L(1, n)$.

End

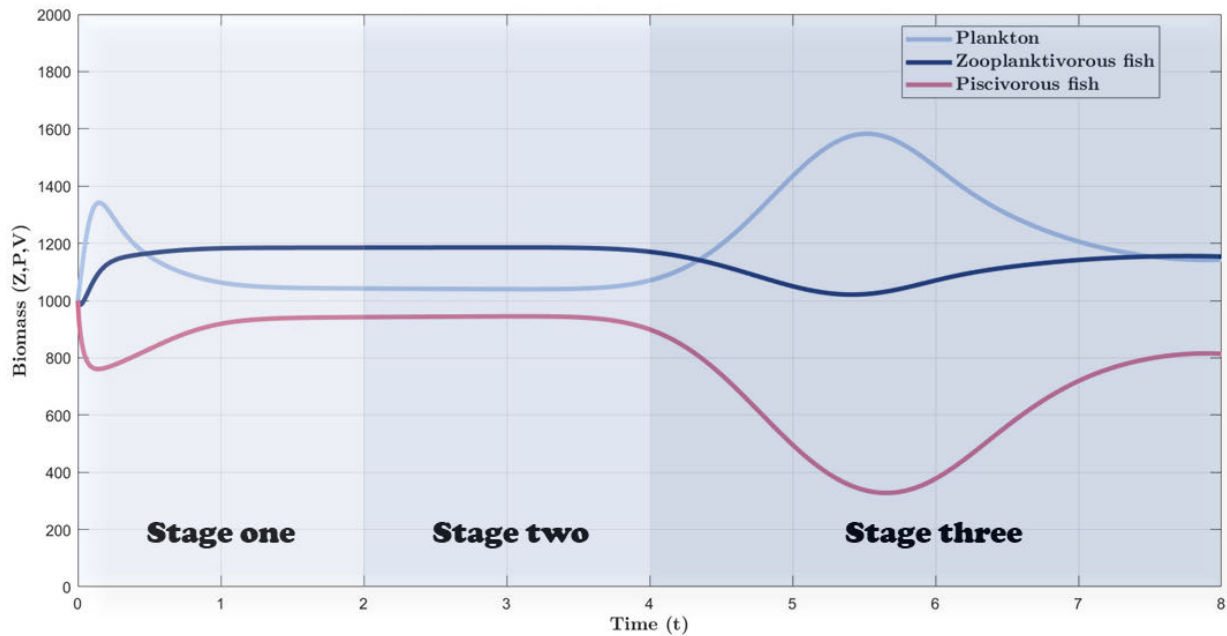


Figure 5: The change of Plankton, Zooplanktivorous fish and Piscivorous fish over time

In figure 5, three categories exemplify the most basic *Lotka-Voterra system* of competitive relationships. We can analyze the whole process in three stages as follows. In Stage one, the number of plankton rises sharply and then drop dramatically. In contrast, the number of Piscivorous fish decrease at first and then ascend quickly. They both eventually stabilised in this stage, and the zooplanktivorous fish have the numerical advantage. In Stage two, three categories keep stable, and there is no change in competitive dominance. In Stage three, the trend of curve is extremely similar to stage one, so we can deduce that it is the beginning of a new cycle.

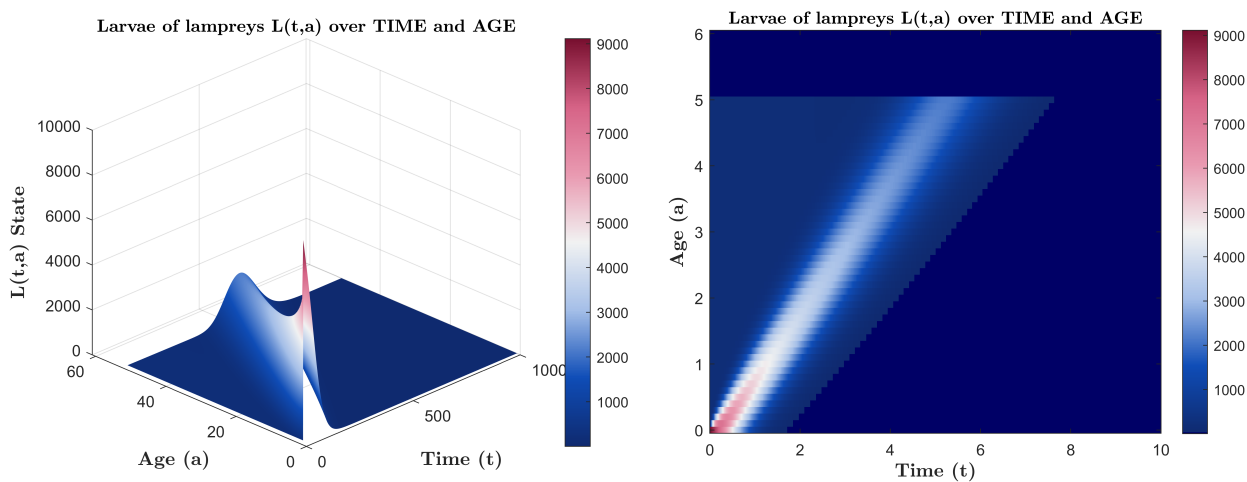


Figure 6: The change of larvae of lampreys $L(t, a)$ over time and age

In figure 6, it is obvious that if age a is ranging from 5 to 6, the number of larvae is 0, which means lampreys will be mature with the availability of spawning and attacking other species at the age of 5. Besides, the number of larvae peaks once over time and then decreases to nearly regional extinction for each age groups. Thus, we can deduce that adult lampreys are far less than the larval ones.

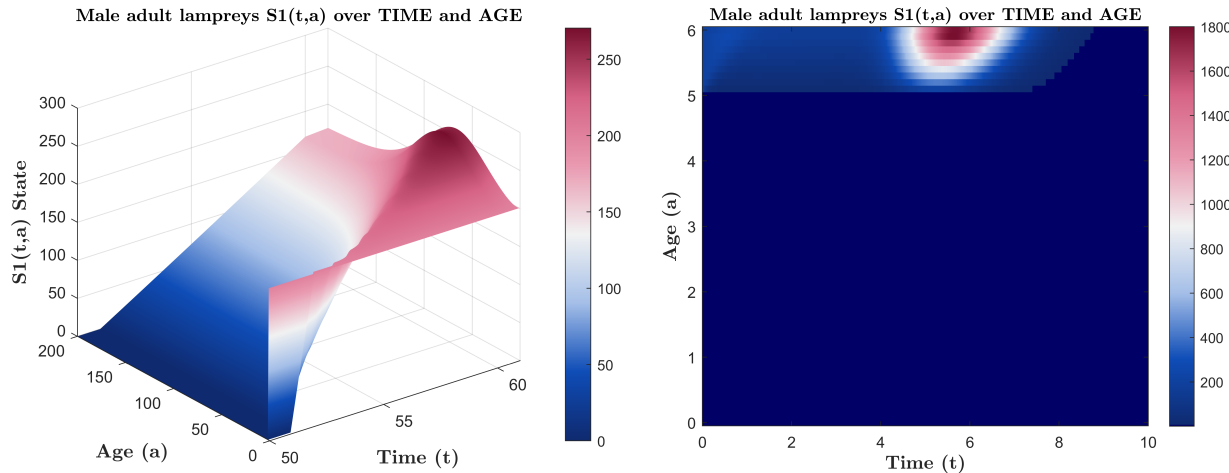


Figure 7: The change of male adult lampreys $S^{(1)}(t, a)$ over time and age

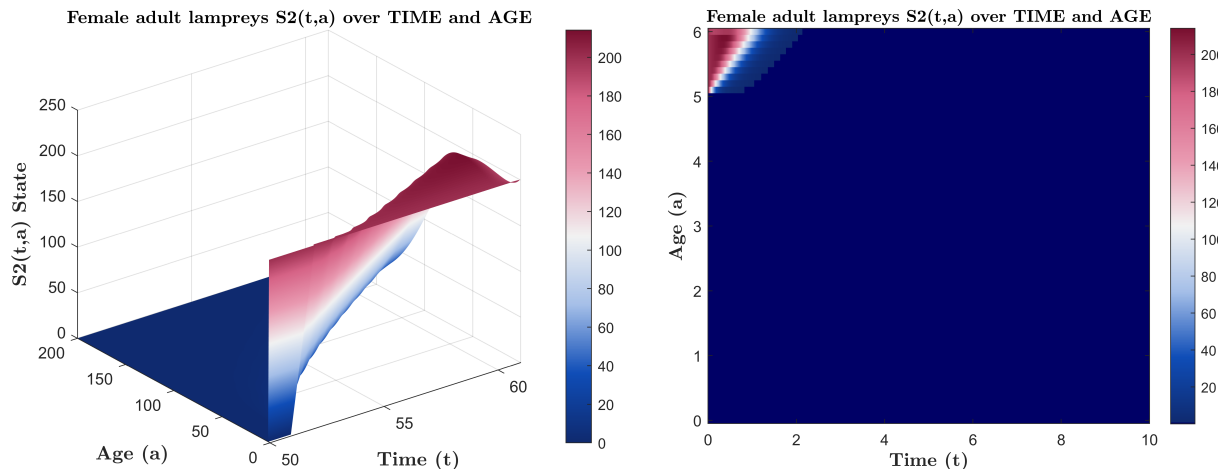


Figure 8: The change of female adult lampreys $S^{(2)}(t, a)$ over time and age

In figure 7, it is obvious that if age a is ranging from 0 to 5, the number of adult lamprey is 0, which satisfies our model assumption 2. Besides, the number of larvae peaks once over time and then decreases to nearly regional extinction for each age groups. Thus, we can deduce that lampreys are not suited for long-term survival in multi-species ecosystems without human factors.

In figure 8, it is obvious that female lampreys are also not suited for long-term survival in multi-species ecosystem. Compared to the male lampreys, female lampreys follow the same trend as males, but they have a shorter survival period due to the high risk of spawning.

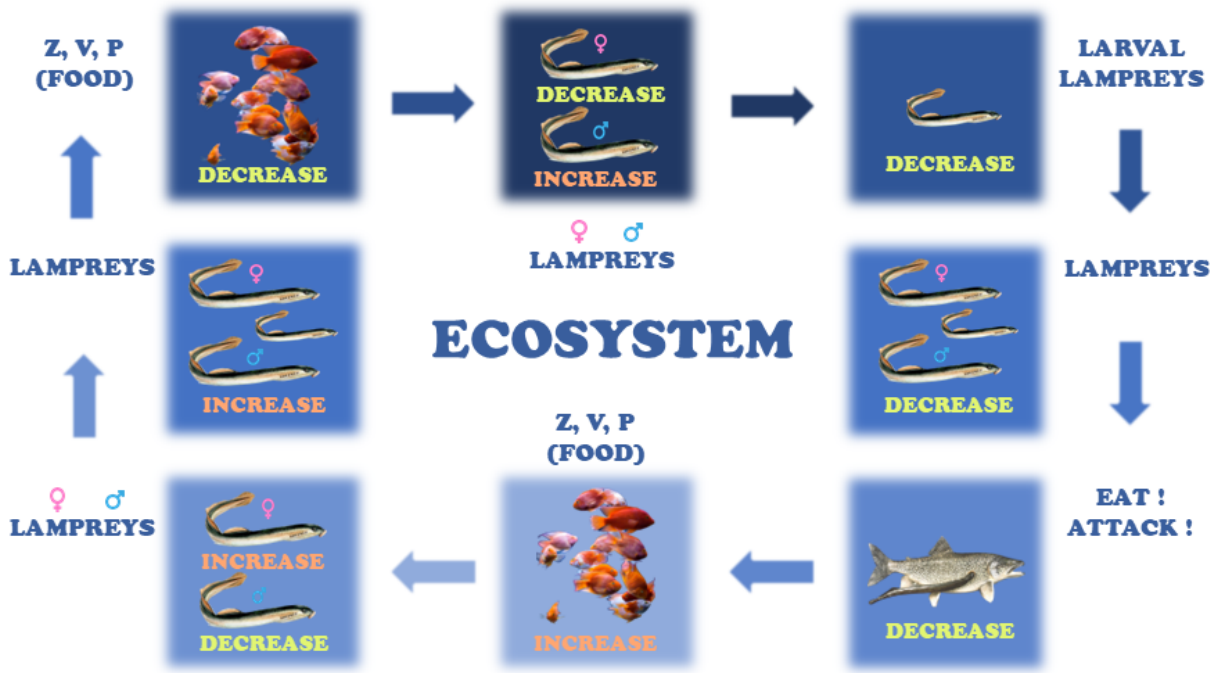


Figure 9: Qualitative analysis of ecosystem steady state

As shown in figure 9, the ecosystem with lampreys and other fishes is a closed loop with balance point, which we will discuss in section 5.

In the ecosystem, as food decreases, the percentage of male lampreys will elevate, which will result in a more imbalanced sex ratio. Lower spawning from the imbalance will lead to a decrease in the overall lampreys population. So mature lampreys will be less aggressive towards other species, allowing the overall ecosystem to increase in species richness, which is one of the benefits of a reduction in lamprey numbers. As more food is available, the proportion of female lampreys and the overall number of lampreys rises, so the food decreases again, thus the ecosystem forms a complete closed loop. However, besides the advantages, a decline in the number of lampreys can also have some bad effects on the ecosystem, which can lead to uncontrolled populations of certain species and thus overpopulation.

5 Equilibrium Points and the Steady States

5.1 Derivation of Trivial and Semi-trivial Equilibrium Points

In this part, following the results in section 4.3, the trivial and semi-trivial equilibrium points of dynamics (8) are derived theoretically.

There are two methods to analyze the stability of the age-structured model: Integrated semi-group^[8] and the characteristic equation and lines method. The latter one is used in this part. As for the proof global stability, a suitable Lyapunov function^[9] can be constructed, but it will not be presented in this paper.

To make the equation more concise, we replace the original subscripts $z, p, v, l, s^{(1)}$ and $s^{(2)}$ with number 1 to 6 respectively. Besides, function $L(t, a)$, $S^{(1)}(t, a)$, and $S^{(2)}(t, a)$ are extension to $(0, +\infty) \times [0, A_2]$. Denote $M(t) = L(t, 0)$.

The equilibrium points of dynamics (8) satisfies the following equations:

$$\left\{ \begin{array}{l} (r_1 - \mu_1)Z^* - \frac{r_1}{K_1}(Z^*)^2 - \sigma_{21}Z^*P^* = 0, \\ (r_2 - \mu_2)P^* - \frac{r_2}{K_2}(P^*)^2 - \sigma_{32}P^*V^* - P^* \left[\sigma_{52} \int_{A_1}^{A_2} S^{*(1)}(a)da + \sigma_{62} \int_{A_1}^{A_2} S^{*(2)}(a)da \right] = 0, \\ (r_3 - \mu_3)V^* - \frac{r_3}{K_3}(V^*)^2 - V^* \left[\sigma_{53} \int_{A_1}^{A_2} S^{*(1)}(a)da + \sigma_{63} \int_{A_1}^{A_2} S^{*(2)}(a)da \right] = 0, \\ \frac{dL^*(a)}{da} = -\mu_4 \cdot L^*(a), \\ \frac{dS^{*(1)}(a)}{da} = F(P^*, V^*) \cdot L^*(A_1) - \mu_5(a) \cdot S^{*(1)}(a), \\ \frac{dS^{*(2)}(a)}{da} = (1 - F(P^*, V^*)) \cdot L^*(A_1) - \mu_6(a) \cdot S^{*(2)}(a), \\ M^* = \varepsilon \int_{A_1}^{A_2} \beta(a)S^{*(2)}(a)da. \end{array} \right. \quad (10)$$

Dynamics (8) always exist a trivial equilibrium point E_0 :

$$\{Z^*, P^*, V^*, L^*(a), S^{*(1)}(a), S^{*(2)}(a)\} = \{0, 0, 0, 0, 0, 0\},$$

which means the extinction of all species in the region.

At the same time, dynamics (8) have at least eight semi-trivial equilibrium points. We divide them into two categories: systems that are not affected by the number of lampreys (11)-(15) and systems that are not affected by the biomass of other species (16). Denote $F_0 = F(0, 0)$.

$$E_1 : \left\{ \frac{(r_1 - \mu_1)K_1}{r_1}, 0, 0, 0, 0, 0 \right\}, \quad E_2 : \left\{ 0, \frac{(r_2 - \mu_2)K_2}{r_2}, 0, 0, 0, 0 \right\}, \quad E_3 : \left\{ 0, 0, \frac{(r_3 - \mu_3)K_3}{r_3}, 0, 0, 0 \right\}, \quad (11)$$

$$E_4 : \left\{ \frac{r_2(r_1 - \mu_1)K_1 - (r_2 - \mu_2)K_1K_2\sigma_{21}}{r_1r_2}, \frac{(r_2 - \mu_2)K_2}{r_2}, 0, 0, 0, 0 \right\}, \quad (12)$$

$$E_5 : \left\{ \frac{(r_1 - \mu_1)K_1}{r_1}, 0, \frac{(r_3 - \mu_3)K_3}{r_3}, 0, 0, 0 \right\}, \quad (13)$$

$$E_6 : \left\{ 0, \frac{r_3(r_2 - \mu_2)K_2 - (r_3 - \mu_3)K_2K_3\sigma_{32}}{r_2r_3}, \frac{(r_3 - \mu_3)K_3}{r_3}, 0, 0, 0 \right\}, \quad (14)$$

$$E_7 : \left\{ \frac{r_2r_3(r_1 - \mu_1)K_1 - (r_2 - \mu_2)r_2r_3K_1\sigma_{21} + (r_3 - \mu_3)K_1K_2K_3\sigma_{32}\sigma_{21}}{r_1r_2r_3}, \right. \\ \left. \frac{r_3(r_2 - \mu_2)K_2 - (r_3 - \mu_3)K_2K_3\sigma_{32}}{r_2r_3}, \frac{(r_3 - \mu_3)K_3}{r_3}, 0, 0, 0 \right\}, \quad (15)$$

$$E_8 : \{0, 0, 0, M^*e^{-\mu_4 a}, F_0 \cdot L^*(A_1) \cdot \Psi_1, (1 - F_0) \cdot L^*(A_1) \cdot \Psi_2\}, \quad (16)$$

where $\Psi_i = e^{-\int \mu_{i+4}(a)da} \left[\int e^{\int \mu_{i+4}(a)da} da + c_i \right]$. (c_i is a constant)

Due to the complexity of the system, it is difficult to give out the non-trivial equilibrium points, but what is known is that a non-zero equilibrium point must be a non-zero solution to the equations (10). Solving non-trivial equilibrium points through numerical methods is the main point of next section 5.2.

5.2 Non-trivial Equilibrium Points and Phase Diagram

In this part, Levenberg-Marquardt algorithm and Trust Region Policy Optimization algorithm are applied to solve the semi-trivial equilibrium points numerically, and it verifies the theoretical results in section 5.1. In addition, we draw its phase diagrams and discuss the special nontrivial equilibrium points when the age function is a constant.

Here we only simulate two typical semi-trivial equilibrium points: the number of lampreys is 0 (Case 1) and the other biomass is 0 (Case 2). The specific semi-trivial equilibrium points are as follows:

Table 4: Two typical semi-trivial equilibrium points

	Z^*	P^*	V^*	L^*	$S^{*(1)}$	$S^{*(2)}$
Case 1	1574.6	1093.6	995.0	0	0	0
Case 2	0	0	0	115.03	1315.4	4601.8

In figure 10, it is obvious that the trajectories converge to specific singular points, which satisfies the numerical solution in table 4. Since a two-dimensional phase

diagram can only describe two dimensions, we use different color to distinguish the direction in third dimension.

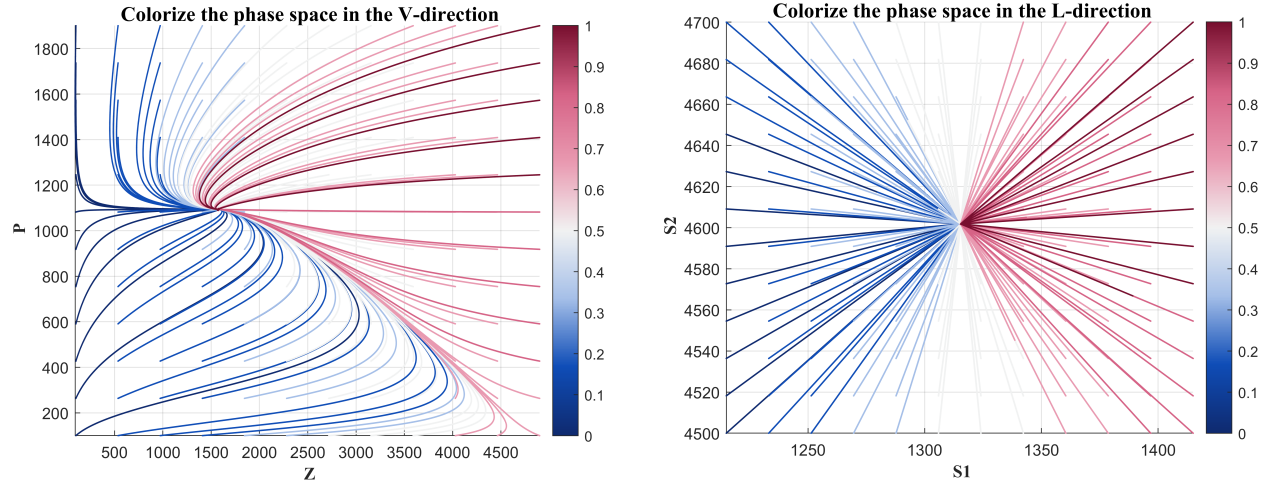


Figure 10: The phase diagram of semi-trivial equilibrium points: Case 1 (left) and Case 2 (right)

By existence and uniqueness theorem for ordinary differential system and extension of solutions, the solution of equations (10) must exist and unique. However, since the system is complicated enough, the method of constructing Lyapunov functions fails to find non-trivial equilibrium points. Taking a step back, we fixed the variation in adult lampreys (*i.e.* set as a constant value function). The possible non-trivial equilibrium points are shown in table 5 below:

Table 5: Several possible non-trivial equilibrium points

No.	Z^*	P^*	V^*	$L^*(a)$	$S^{*(1)}(a)$	$S^{*(2)}(a)$
1	935.40	1298.2	745.00	$12\varepsilon \cdot e^{-0.05a}$	13.00	12.00
2	833.10	1330.9	705.00	$6\varepsilon \cdot e^{-0.05a}$	23.00	6.00
3	986.50	1281.8	765.00	$5\varepsilon \cdot e^{-0.05a}$	18.00	5.00
4	884.20	1314.5	725.00	$17\varepsilon \cdot e^{-0.05a}$	10.00	17.00
5	449.60	1453.6	555.00	$19\varepsilon \cdot e^{-0.05a}$	25.00	19.00
6	142.80	1551.8	435.00	$22\varepsilon \cdot e^{-0.05a}$	34.00	22.00

Note: $\varepsilon = 12$. $S^{*(1)}(a)$ and $S^{*(2)}(a)$ are constant function.

In addition to equilibrium points, asymptotic smoothness and Hopf branches are also the key to obtaining global properties, but this is not the focus of this paper. When A_1 is sufficiently large, stable periodic solutions or stable steady state solutions are observed. The relevant theory can be found in [10].

6 Parasite Distribution Dynamics with Diffusion Terms

6.1 Sex Ratio and Parasite Distribution Model

In this part, we consider the relationship between parasites and sex ratio in lamprey population as figure 11 shown. Based on the original dynamics (8), we add a two-dimensional second-order partial differential equation to represent the diffusion effect of the parasite under different sex ratios.

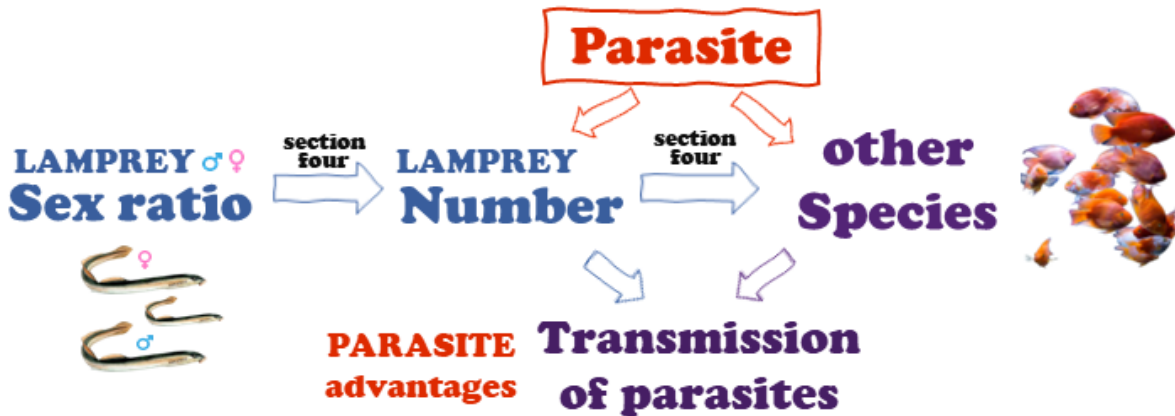


Figure 11: The transmission of parasites (schematic diagram)

By **assumption 3**, for the parasitic lamprey, in the larval stage it will be in close contact with sediments in fresh water. Most larvae form burrows in fine sediments and filter feed on diatoms and other freshwater particulates. After maturity, it will parasitize other species and feed on the blood and flesh of the host. Because microbes may be encountered in both freshwater sediments and host body fluids, lamprey potentially are exposed to a broader range of pathogens than other aquatic species^[11]. Therefore, the presence of lamprey encourages the spread of parasites.

Consider the following two-dimensional dynamics with diffusion terms:

$$\begin{cases} \text{Dynamics (8)}, \\ \frac{\partial u}{\partial t} - G(Z(t), P(t), V(t)) \cdot \left(\frac{\partial^2 u}{\partial x^2} + \frac{\partial^2 u}{\partial y^2} \right) = 0, \quad (x, y) \in \Omega, \end{cases} \quad (17)$$

where

$u(x, y, t)$ is the density of parasites at (x, y) at time t ;

G is a diffusion coefficient determined by $Z(t), P(t), V(t)$ mentioned in dynamics (8).

Suppose that function $u(x, y, t)$ has the second continuous partial derivatives for all independent variables. We also assume that region Ω is bounded which can be denoted as $[-a, a] \times [-a, a]$ ($a > 0$).

In order to explore the diffusion effect of parasites, we give the density at the centre of the region at the initial moment, and the density at the boundary of the region to be the Dirichlet boundary value condition. The specific expression is as follows:

$$\begin{cases} u|_{|x|=a} = u|_{|y|=a} = 0, \\ u|_{t=0} = a - \sqrt{x^2 + y^2}, & x^2 + y^2 \leq a^2, \\ u|_{t=0} = 0, & x^2 + y^2 > a^2. \end{cases}$$

The solution of dynamics (17) can be obtained by Fourier transform, and then according to the principle of extreme value, the uniqueness and stability of the solution of this system can be obtained easily.

6.2 Numerical Simulation and Chebyshev Spectral Method

In this part, *Chebyshev Spectral Method*^[12] is applied to solve the parasite dynamics with diffusion terms and we analyze the visualisation results. This method has high accuracy and fewer coefficients and is well suited to be used for simulation. To solve for the dynamical system (17), we indicate the values of the discretized function at locations other than the boundary by the square matrix $\tilde{\mathbf{u}}_{(N-1) \times (N-1)}$:

$$\tilde{\mathbf{u}}_{(N-1) \times (N-1)} = \begin{pmatrix} u_{11} & u_{12} & \cdots & u_{1(N-1)} \\ u_{21} & u_{22} & \cdots & u_{2(N-1)} \\ \vdots & \vdots & \ddots & \vdots \\ u_{(N-1)1} & u_{(N-1)2} & \cdots & u_{(N-1)(N-1)} \end{pmatrix}.$$

Then, we have

$$\frac{\partial^2 u}{\partial y^2} \rightarrow \tilde{\mathbf{D}}_N^2 \tilde{\mathbf{u}}_{(N-1) \times (N-1)}, \quad (18)$$

$$\frac{\partial^2 u}{\partial x^2} \rightarrow \left(\tilde{\mathbf{D}}_N^2 (\tilde{\mathbf{u}}_{(N-1) \times (N-1)})^T \right)^T = \tilde{\mathbf{u}}_{(N-1) \times (N-1)} \left(\tilde{\mathbf{D}}_N^2 \right)^T, \quad (19)$$

where D_n is *Chebyshev Derivative Matrix*.

Next, we assigned values to the parameters:

Table 6: **Parametric description and their values**

Parameter	Description	Values	Sources
a	absolute value of the length of the region's sides	2	assumed

Table 7: **Illustration of the MATLAB Simulation****Input:**Parameters: a Initial value conditions: $u|_{t=0} = a - \sqrt{x^2 + y^2}$

- **function** [D,x]= cheb (N)

- **If:** N==0

- Output a 0 matrix D and a vector x with 1 element.

- **Return**

- Construct a Chebyshev differential matrix D and Chebyshev nodes x .

- **End function**

Main script:

- Call the cheb function to generate the Chebyshev differential matrix D and the Chebyshev node x .

- Adjust the length of the matrix interval.

- Get the second order derivative matrix.

- Apply boundary conditions to internal sub matrices.

- Adjust Chebyshev node x from the standard interval to a physical interval of length L.

- Generate a 2D mesh using internal nodes.

- End**

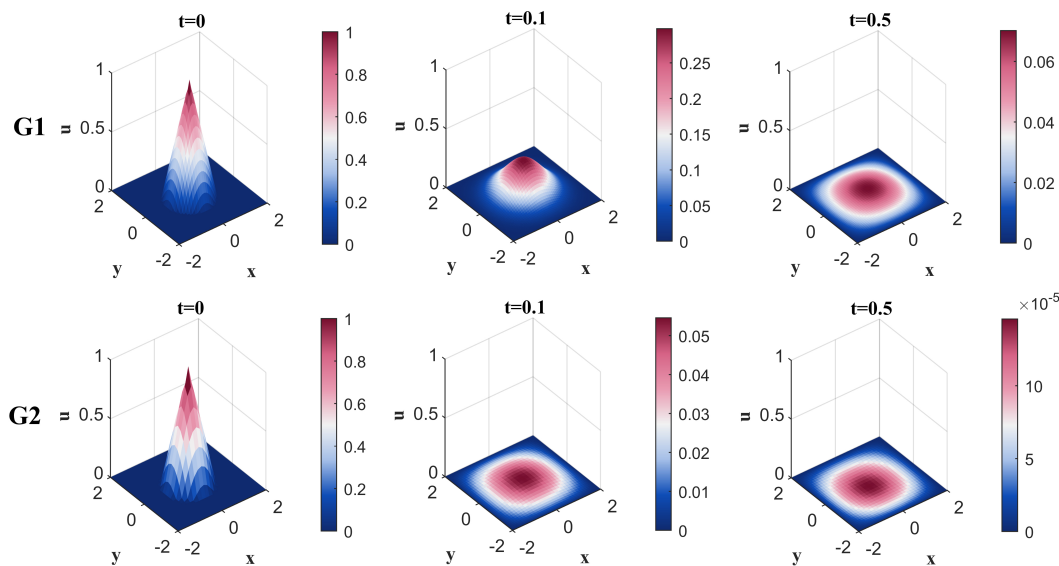


Figure 12: Spread of parasites with different diffusion coefficients

In figure 12, it reflects the different effects caused by two different diffusion coefficients, the bottom row G_2 has a larger diffusion coefficient than the top row G_1 . Clearly, the diffusion rate is positively correlated with the diffusion coefficient. Besides, the density field tends to stabilize over a long period of time, i.e. the dynamics can be transformed into Laplace equation.

7 Sensitivity Analysis and Model Testing

In this section, we analyze the sensitivity of the dynamics (17) when its initial-boundary value conditions are changing. In other words, we deal with whether high or low initial parasite density has a significant effect on diffusion.

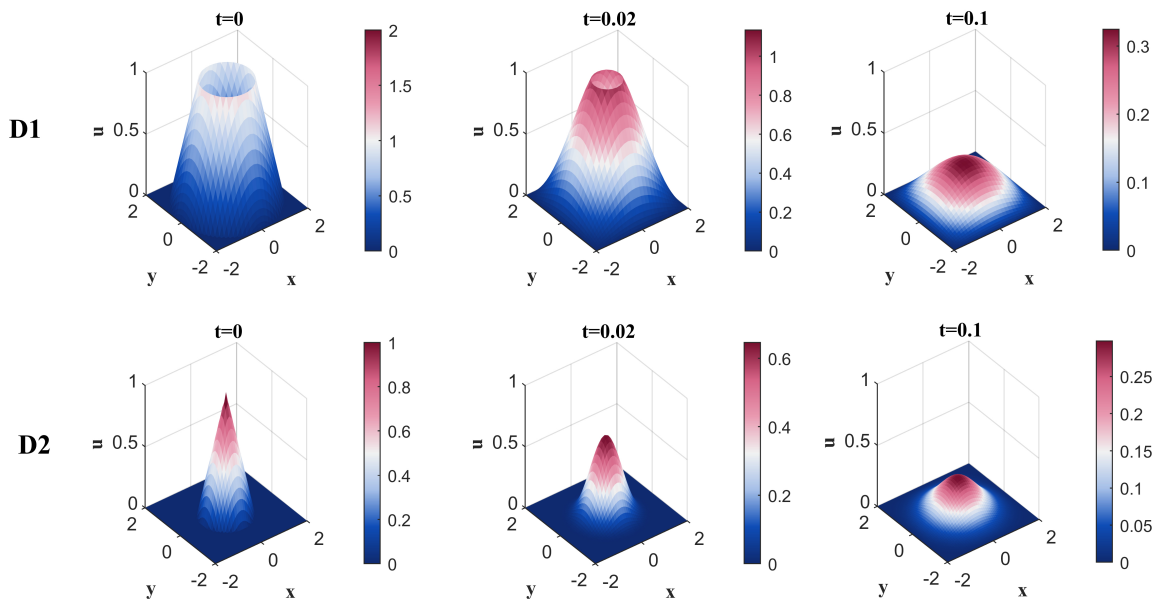


Figure 13: Spread of parasites with different initial-boundary value conditions

In figure 13, the top row D_1 represents a higher initial density. It is clear that the level of parasite density is strongly related to the initial value conditions, and the larger the initial value conditions, the higher the density in the whole solution space.

The National Oceanic and Atmospheric Administration website contains zooplankton biomass data ² during 2010-2019 from different monitoring sites in the Great Lakes. If this data set is combined with the data set about sex ratio of lampreys mentioned in this paper, the accuracy of the fitting function given in section 4.2 can be verified.

Without giving the specific process of testing, determination coefficient $R^2 = 0.9353$, but the fitting of fluctuation data in short stage needs to be further improved.

²<https://www.nodc.noaa.gov/archive/arc0208/0260131/1.1/data/0-data/to-ncei/> accessed on Feb. 6th, 2024

8 Strengths and Weaknesses

8.1 Strengths

- 1) The age structure of the lampreys is considered in the holistic ecosystem dynamics and diffusion terms are added into the sex ratio and parasite distribution model, which is more in line with the real situation.
- 2) Polynomial regression and support vector machines are both applied comparatively in determining the sex ratio function; meanwhile, Levenberg-Marquardt algorithm and Trust Region Policy Optimization algorithm both excelled in terms of convergence speed when solving for non-trivial equilibrium points.
- 3) We make good use of the *Chebyshev Spectral Method* in section 6, which is highly efficient for solving smooth problems due to the fast convergence of Chebyshev polynomials, achieving high accuracy with fewer coefficients.

8.2 Weaknesses

- 1) The dynamics are too complicated, resulting in many global properties that can only be given by numerical methods. (*e.g.* non-trivial equilibrium points)
- 2) In section 6, we have only considered the case of parasites transmitted by lamprey that are parasitic when mature, and have not split the situation to consider the case of lamprey that are non-parasitic (brook).
- 3) When solving the sex ratio function, we only use data from the Great Lakes region for the fit; more data could have been collected to make the results more convincing.

9 Future Discussion

According to the latest posted article ^[13], the parasitic and non-parasitic lampreys regulate ionization in different ways during the life cycle. Therefore, they will also behave in many different ways at various stages of the life cycle. We can discuss how each of the two lampreys responds by regulating differently when analyzing the transmission of the parasite.

Additionally, when the lamprey enters the spawning phase and loses its ability to attack, it descends from the top of the food chain and becomes food for others. We can enrich our research analysis of parasite transmission from this perspective.

References

- [1] M. W. Hardisty. Sex composition of lamprey populations. *Nature*, 191(4793):1116–1117, 1961.
- [2] M. W. Hardisty. Duration of the larval period in the brook lamprey (*lampetra planeri*). *Nature*, 167(4236):38–39, 1951.
- [3] N. S. Johnson, T. J. Buchinger, and W. Li. Reproductive ecology of lampreys. *Lampreys: Biology, Conservation and Control: Volume 1*, pages 265–303, 2015.
- [4] M. F. Docker. *Lampreys: biology, conservation and control*. Springer, 2015.
- [5] H. S. Dean. *The growth and development of the system of public bank inspection in the US*. PhD thesis, Cornell University, 1898.
- [6] N. S. Johnson, W. D. Swink, and T. O. Brenden. Field study suggests that sex determination in sea lamprey is directly influenced by larval growth rate. *Proceedings of the Royal Society B: Biological Sciences*, 284(1851):20170262, 2017.
- [7] S.B. Hsu, S. Ruan, and T.H. Yang. Analysis of three species lotka–volterra food web models with omnivory. *Journal of Mathematical Analysis and Applications*, 426(2):659–687, 2015.
- [8] H. R. Thieme. Semiflows generated by lipschitz perturbations of non-densely defined operators. 3(6):1035–1066, 1990.
- [9] H. L. Smith and H. R. Thieme. *Dynamical systems and population persistence*. American Mathematical Soc., 2010.
- [10] Y. Cai, C. Wang, and D. Fan. Bifurcation analysis of a predator–prey model with age structure. *International Journal of Bifurcation and Chaos*, 30(08):2050114, 2020.
- [11] M. A. Shavalier, M. Faisal, M. L. Moser, and T. P. Loch. Parasites and microbial infections of lamprey (order petromyzontiformes berg 1940): a review of existing knowledge and recent studies. *Journal of Great Lakes Research*, 47:S90–S111, 2021.
- [12] P. Agarwal, M. Attary, M. Maghasedi, and P. Kumam. Solving higher-order boundary and initial value problems via chebyshev–spectral method: application in elastic foundation. *Symmetry*, 12(6):987, 2020.
- [13] S. Davidson. Comparing ionoregulation and modes of nitrogen excretion across the life cycle of parasitic and non-parasitic lamprey species. 2024.
- [14] E. Ross. Growth spurts may determine a lamprey’s sex. *Nature*, 2017.

Declaration on the use of AI

It is imperative to emphasize that throughout this entire research endeavor, encompassing model assumptions, model establishment, and model resolution, **no interventions or contributions** from artificial intelligence were employed. This deliberate choice underscores the reliance on traditional research methodologies, ensuring the rigor and autonomy of the study.